

ORIGINAL ARTICLE

The production of a lead glaze with galena: Thermal transformations in the PbS–SiO₂ system

Roberta Di Febo¹  | Judit Molera¹  | Trinitat Pradell²  | Joan C. Melgarejo³  | Josep Madrenas⁴ | Oriol Vallcorba⁵ 

¹U. Science Tech, MECAMAT Group, University of Vic—Central University of Catalonia, Vic, Spain

²Physics Department, UPC-BarcelonaTech, Castelldefels, Spain

³Department of Mineralogia, Petrologia i Geologia Aplicada, University of Barcelona, Barcelona, Spain

⁴Escola d'Art i Superior de Disseny de Vic, Vic, Spain

⁵ALBA Synchrotron Light Source, Barcelona, Spain

Correspondence

Judit Molera, U. Science Tech, MECAMAT Group, University of Vic—Central University of Catalonia-, Vic, Spain.

Email: judit.molera@uvic.cat

Funding information

Generalitat de Catalunya, Grant/Award Number: 2014SGR-1585, 2014SGR-1661, 2014SGR-581; University of Vic—Central University of Catalonia.; Ministerio de Ciencia e Innovación (Spain), Grant/Award Number: MAT2016-77753-R; ALBA Synchrotron Light Facility, Grant/Award Number: 2014060905 (BL04)

Abstract

Galena, also known as PbS, was widely used in the production of lead glazes from the beginning of the 18th century to the second half of the 20th century. Although the PbO–SiO₂ system has been studied for years, the PbS–SiO₂ phase diagram, involved in the formation of a glaze with galena, has not yet been investigated. Temperature transformations for the system 75 wt% PbS–25 wt% SiO₂ are investigated in a high-temperature resolved X-ray diffraction experiment with synchrotron radiation and compared to those of the equivalent system 70 wt% PbO–30 wt% SiO₂. Lanarkite, PbO·PbSO₄, is the phase predominantly formed as soon as galena decomposes during the heating. The results show that the system melts at a temperature higher than the PbO–SiO₂ system, but far lower than those expected for the PbO–PbSO₄–PbS system. A historical misfired lead glaze produced with galena is also studied. The presence of galena, lanarkite, and mattheddleite, Pb₁₀(SiO₄)_{3.5}(SO₄)₂Cl₂, is determined and discussed in terms of the composition of the galena mineral used and the firing conditions in light of the high-temperature transformations previously obtained.

KEYWORDS

2PbO·PbSO₄, 4PbO·PbSO₄ mattheddleite, galena, high lead glazes, PbO·PbSO₄ lanarkite, PbO–SiO₂ system, PbS–SiO₂ system, thermal stability

1 | INTRODUCTION

Lead glazes are among the earliest glazes used to coat earthenware, stoneware, and porcelain to make them waterproof. Lead glazes have a wide processing range, low melting point, low viscosity and surface tension, and a thermal expansion coefficient which match those of earthenware giving them good adherence (minimal flaking and crazing) and excellent covering capability. They also have a high refraction index that confers brilliance to the glaze.¹

The first lead-containing glazes were produced in China (Warring States period, 475–221 BC), to cover large jars,

but were comprised of relatively low quantities of lead (<20 wt% PbO). High lead glazes (with composition close to the eutectic mixture 70 wt% PbO, 30 wt% SiO₂, which melts at 717°C) were not produced until the 1st century BC (Han dynasty and Greco-Roman world).^{2,3} All these glazes show green, yellow, and brown colors and imitated metal forms.⁴

There were two primary methods of applying lead glazes to ceramic surfaces: either using lead compounds alone or a mixture of lead compounds plus powdered quartz or sand.² The former method was used between the 1st and 3rd centuries AD and the latter between the 2nd and 4th centuries AD.⁴ One further variation was the

fritting of the lead compounds-plus-quartz mixture before its application to the ceramic surface.¹ A frit is any glassy or partially glassy material obtained after firing a mixture of sand with flux materials (lead compounds, plant ashes, alkaline salts, etc.).⁵ This method was widely used in the Medieval period until modern times.

Galena, PbS, is the most important lead ore and known to have been widely exploited by the Romans to extract silver and to obtain metallic lead, but there is no archeological evidence or literature demonstrating the use of galena or roasted galena (PbO) in the production of the lead glaze in Roman times. The use of galena would have the advantage of eliminating one stage (the roasting of galena to obtain lead oxide) in the process of producing a lead glaze. However, the use of galena was not documented until the 18th century.⁶ At the same time as Ramazzini, an Italian physician linked the diseases shared by potters, guilders, and glassmakers to lead poisoning.⁷

Although there is a detailed phase diagram for the PbO–SiO₂ system,^{8–10} there is no information about the transformations that take place in the PbS–SiO₂ system. However, complementary information of the Pb–PbS, PbS–O, and PbO–PbSO₄ systems is available.^{11–14} The use of *galena* implies the oxidation of PbS, but as PbS and PbO do not have a common boundary in the phase diagram, it will always involve the formation of lead sulfates and oxysulfates; PbO·PbSO₄, 2PbO·PbSO₄, and 4PbO·PbSO₄ which are known to have a limited solubility in the silica melt. Therefore, the use of galena implies oxidation of the PbS into PbSO₄ and progressively more oxidized oxysulfates, sulfate anion breakdown (above 880°C), and the reaction with SiO₂ to obtain the melt. The main advantage of the PbO–SiO₂ system in the production of glazes is its low melting point (717°C¹⁰). The large compositional range, between 20 and 60 mol% SiO₂, for which a melt forms at a relatively low temperature, below 760°C¹⁰, is also an advantage. This does not occur in the PbS–SiO₂ system. The PbS–PbSO₄–PbO phase diagrams show higher melting temperatures, the lowest for the more oxidized species at 916°C.

The production of a lead glaze with *galena*, PbS–SiO₂ system, and the equivalent PbO–SiO₂ system are investigated in a time-resolved high-temperature X-ray diffraction experiment with synchrotron radiation (HT-SR-XRD). Although the equilibrium phase diagram of the PbO–SiO₂ system is well known, equilibrium conditions are not necessarily reached during the time-resolved experiment. Therefore, the data obtained for the PbO–SiO₂ mixture will reveal any shift in the phase transformation and melting temperatures due to nonequilibrium conditions.

A historical misfired lead glaze ware that retains *galena* relic grains is also studied. The crystalline phases present in the glaze vestiges from an incomplete glaze firing are identified, and their presence is discussed in terms of the

data obtained from the high-temperature experiment and of the composition of the glaze. Finally, the reasons for the use of galena in the production of lead glazes and its limitations are discussed in light of the results obtained.

2 | EXPERIMENTAL PROCEDURE

2.1 | High-temperature resolved XRD experiment (HT-SR-XRD)

Two mixtures of the eutectic composition 70 wt% PbO:30 wt% SiO₂ were prepared using PbO in one case and using galena in the second case. Chemical reagents for both the PbO (Fluka ref. 11526) and SiO₂ (Merck ref. 107536) were selected. Galena is of mineral origin, and the sample obtained was from the Molar mine (Catalonia).

The in situ high-temperature X-ray diffraction measurements were obtained on the high-brilliance, high-energy (90 keV) (HT-SR-XRD) synchrotron beamline ID15B at the ESRF (Grenoble, France). The experimental setup consisted of a small cylindrical furnace with the raw powders contained in unsealed 0.5-mm-diameter MgO capillaries mounted on a goniometer for alignment. An image-plate detector (Model MAR345; Marresearch, Norderstedt, Germany) was used to collect the XRD patterns with an exposure time of 1 min, and rotation of the sample was sufficient to ensure good data quality.

The furnace temperature was controlled by a previously calibrated external regulator. An initial drying stage was programmed, consisting of a slow heating rate (1°C/min) between 90 and 110°C and then maintaining the temperature for 5 min. The sample was afterward heated at a constant heating rate of 5°C/min up to the maximum temperature with data being recorded during this slow ramping. The measuring time took only 1 min and consequently a variation of 5°C existed between the beginning and the end of the data collection. The data collection, readout, and erasure of the image plate took 4 min in total. The whole cycle for each dataset took 5 min (measuring time, readout, and then erasure of the image plate), resulting in images being taken every 25°C. Finally, the sample was cooled down to room temperature at a rate of 10°C/min. The whole measurement cycle took 3 h.

The calibration of the sample to detector distance, beam center, and orthogonality of the detector was determined using a silicon standard measured under the same conditions. The radial integration of the images was performed using the Fit2D software.¹⁵ Identification of the compounds was performed based on the powder diffraction file (PDF) database from the International Centre for Diffraction Data (ICDD). Figures 2 and 3 represent high-temperature XRD patterns (HT-SR-XRD) obtained during the firing of the mixtures. Thermal stability ranges of the crystalline phases

identified for (a) PbO-SiO_2 and (b) PbS-SiO_2 are shown in Figure 4. The ordinate axis is obtained from the intensity of the principal peak of each crystalline phase relative to the intensity of the MgO crucible and gives a qualitative temperature evolution of each compound.

2.2 | Analysis of a misfired glaze

A misfired storage jar (CCV050) dating from the 18th century was investigated.⁶ The jar was part of an assemblage of coarse wares found in the garret of *Casa Convalescència*, an ancient hospital building that provided medical assistance, in Vic. Due to uncontrolled and unequal temperature conditions in the kiln, the glaze exhibits three different colors: opaque green, opalescent yellow, and transparent honey (Figure 1).

A polished thin section of glaze and ceramic body to a standard thickness of $30\ \mu\text{m}$ was obtained. The thin section was studied by optical microscopy (OM) with transmitted and reflected light using a petrographic microscope (LEICA DM 2700 P; Leica Microsystems, Wetzlar, Germany) and scanning electron microscopy with an energy dispersive spectroscopy detector attached (SEM-EDS) to identify the crystalline compounds present. A crossbeam

workstation (Zeiss Neon 40; Carl Zeiss AG, Oberkochen, Germany) equipped with a Schottky field emitter column with an EDS detector (INCAPentaFETx3 detector, $30\ \text{mm}^2$, ATW2 window, Oxford Instruments, Abingdon, UK) attached was employed for the SEM investigation. Backscattered electron (BSE) images were obtained and analyses of the crystallites were carried out to ascertain the composition at 20 kV acceleration voltage.

Electron microprobe (EPM, JEOL JXA-8230; JEOL Ltd, Akishima, Tokyo, Japan) was also used to quantify the chemical composition of the different microcrystallites present that contained both Pb and S which requires the high-energy resolution provided by the WDS (wavelength dispersive spectroscopy) detector. A minimum of three analyses of the crystallites and of the glaze were acquired, and the average and standard deviation were obtained. The operating conditions were 20 kV and 15 nA with a focused beam (spot analysis). The standards used were PbS for galena and Pb, SrSO_4 for S, CaSiO_3 for Si and Ca, and AgCl for Cl. Finally, the chemical composition of the glaze was determined avoiding the glaze-ceramic interface as well as the crystallites.

The crystalline structure of the microcrystallites was determined by synchrotron radiation micro-X-ray diffraction

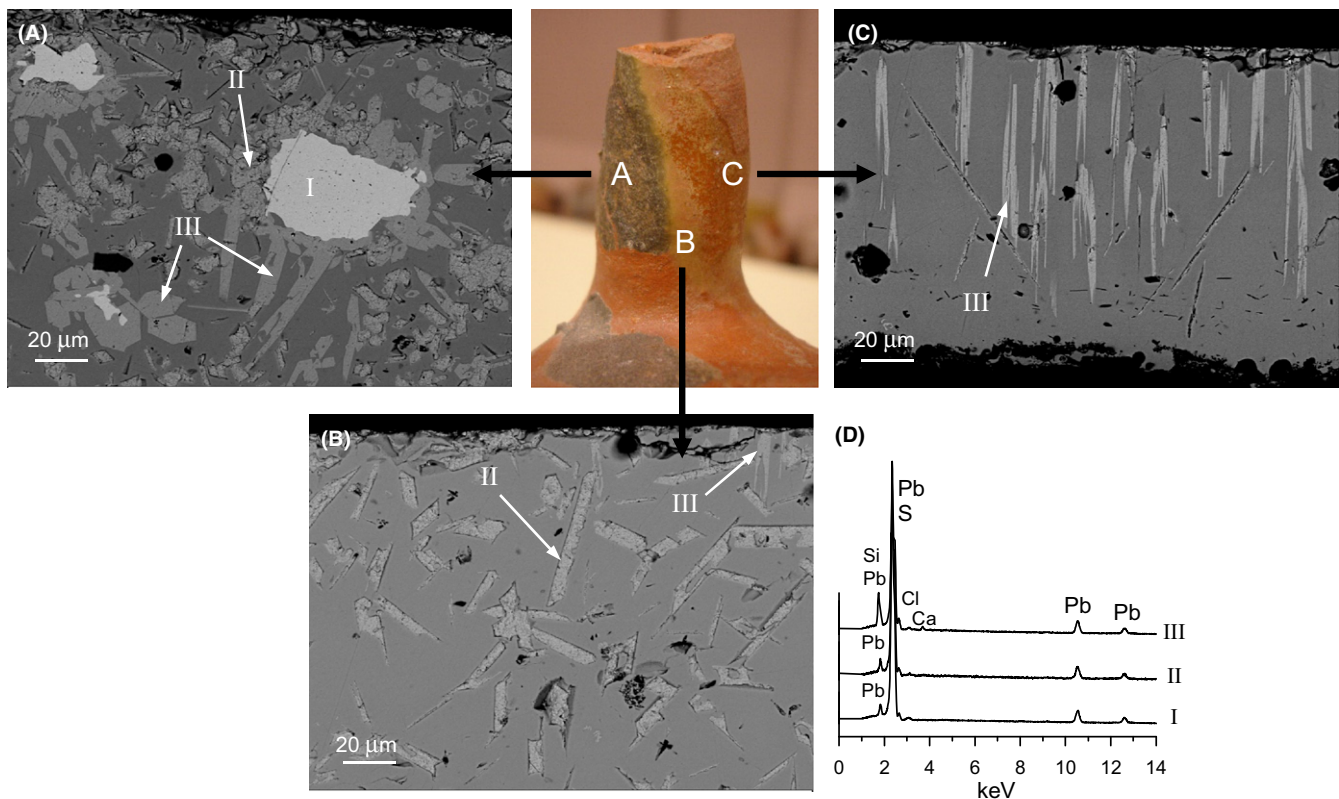


FIGURE 1 The neck of a 18th-century jar, which exhibit a misfired glaze showing three color glaze areas. Scanning electron microscopy backscattering images of (A) the opaque green area which contains relics of galena (I) and neoformed crystallites II and III, (B) the translucent yellow area containing crystallites II and III, and (C) the honey transparent area containing only crystallites III. (D) EDS spectra of the three types of crystallites

(SR- μ XRD) on the same polished thin section in the focused beam station of beamline BL04¹⁶ at the ALBA Synchrotron (Spain). The areas of interest from the polished thin section were selected using an on-axis visualization system and measured in transmission geometry with a $15 \times 15 \mu\text{m}^2$ (FWHM) focused beam of 29.2 keV ($\lambda = 0.4246 \text{ \AA}$). The diffraction patterns were recorded with a Rayonix SX165 CCD detector (active area of 165 mm diameter, frame size 2048×2048 pixels, $79 \mu\text{m}$ pixel size, and dynamic range 16 bit). The calibration of the sample to detector distance, beam center, and orthogonality of the detector were performed using a LaB_6 standard, and the radial integration of the images was performed with the Fit2D software.¹⁵ Identification of the compounds was performed based on the powder diffraction file (PDF) database from the ICDD.

3 | RESULTS

The corresponding high-temperature diffraction data taken during the heating of PbO-SiO_2 and PbS-SiO_2 mixtures are shown in 2D images in Figures 2 and 3, respectively. The HT-SR-XRD patterns taken before heating and after cooling are also shown. Apart from the initial and new

crystalline compounds formed during the heating, the XRD pattern corresponding to the periclase (MgO) from the crucible is also seen.

3.1 | PbO-SiO_2 high-temperature resolved XRD experiment

The high-temperature diffraction data taken during the heating of a mixture 70 wt% PbO : 30 wt% SiO_2 is shown in Figure 2 and the appearance and disappearance of the phases marked. The initial compounds are massicot (PbO , orthorhombic, Pbcm) and α -quartz (SiO_2 , trigonal). The thermal stability range of the different compounds identified is summarized in Figure 4A.

The reversible transformation between α - SiO_2 and β - SiO_2 at 573°C is observed in Figure 2. PbO was stable up to 560°C . At 600°C , PbO began to decrease until it disappeared completely at 722°C . A melt coexisting with other crystalline compounds (a melt is expected to form at 717°C ¹⁰ in the system 70 wt% PbO -30 wt% SiO_2) was clearly found at about 722°C . As soon as PbO reacted with SiO_2 , Pb_2SiO_4 was formed increasing until 690°C ; it decreased quickly at 715°C and completely disappeared at 727°C . At 670°C , Pb_4SiO_6 was formed and disappeared at 722°C . Finally, PbSiO_3 was formed at 625°C and

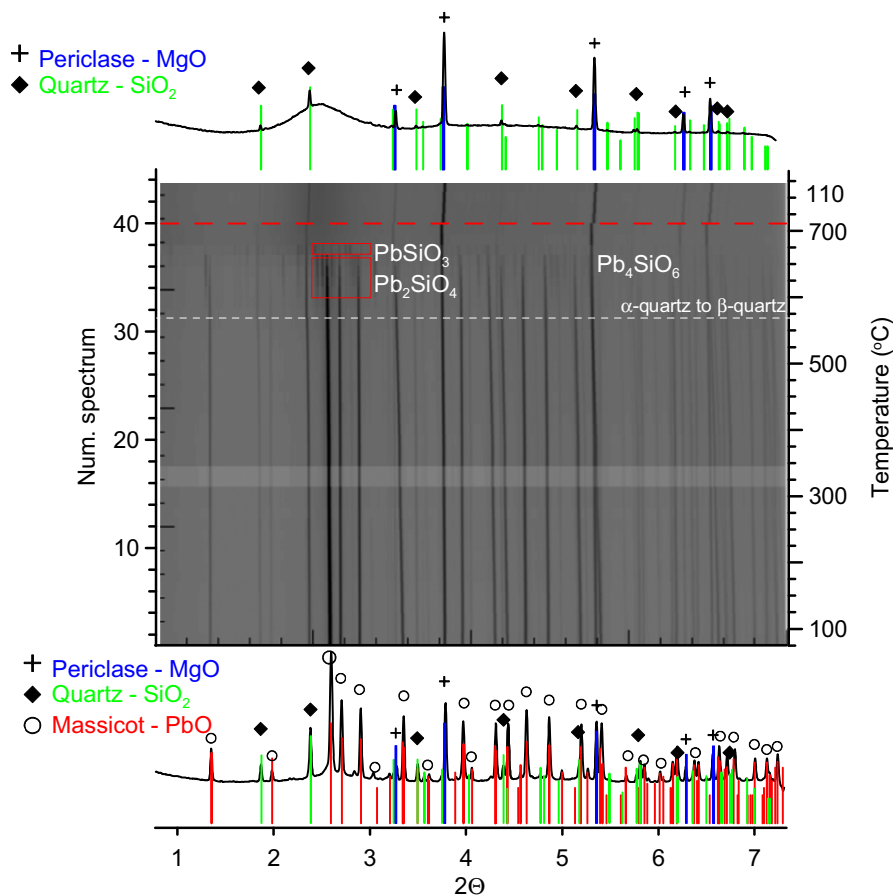


FIGURE 2 High-temperature XRD patterns (HT-SR-XRD) obtained during the firing of 70 wt% PbO -30 wt% SiO_2 . The XRD patterns corresponding to the initial mixture before heating (bottom) and after cooling (top) are also shown

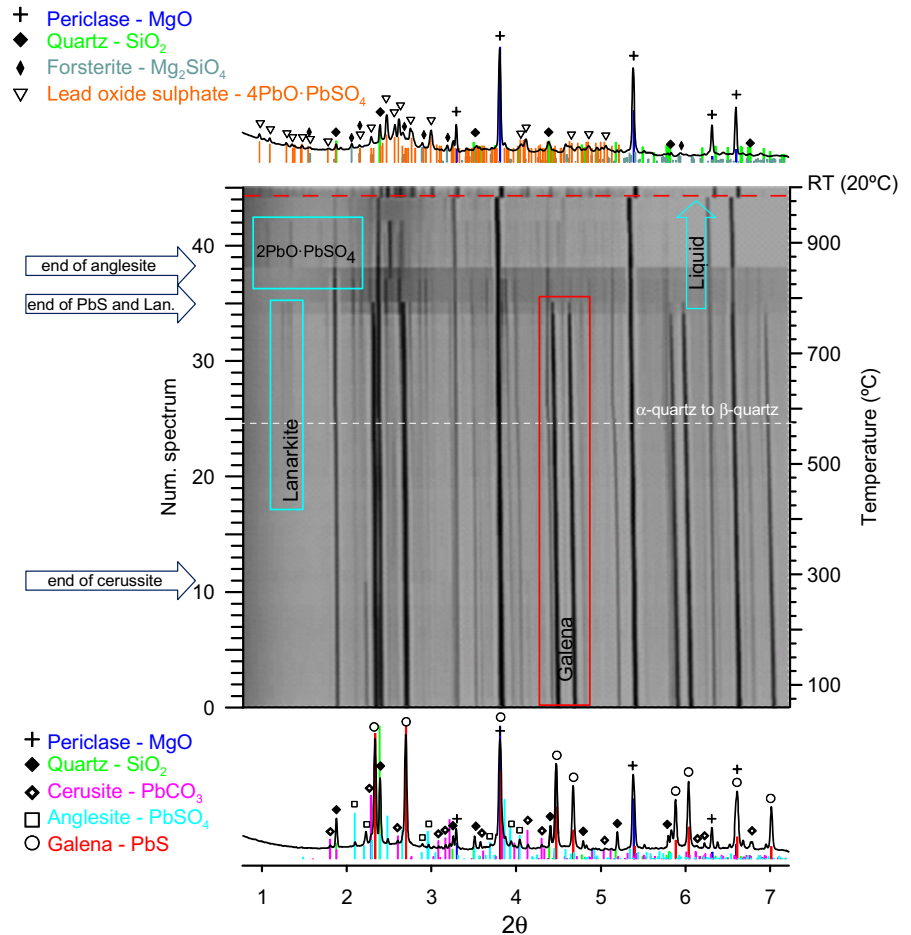


FIGURE 3 High-temperature XRD patterns (HT-SR-XRD) obtained during the firing of the mixture 75 wt% PbS-30 wt% SiO₂. The XRD patterns corresponding to the initial mixture before heating (bottom) and after cooling (top) are also shown

disappeared completely at 727°C with an increase in the range 715-722°C, just when Pb₄SiO₆ decomposed incongruently into Pb₂SiO₄ and PbSiO₃.

3.2 | High-temperature resolved XRD experiment PbS-SiO₂

The high-temperature diffraction data obtained for a mixture of 75 wt% of galena plus 30 wt% of quartz with a composition equivalent to the eutectic composition 70 wt% PbO:30 wt% SiO₂ are shown in Figure 3. The appearance and disappearance of the phases are also marked. The initial compounds determined were galena (PbS), α-quartz, anglesite (PbSO₄), cerussite (PbCO₃), as well as periclase (MgO) from the crucible. Both anglesite and cerussite are weathering compounds of the natural galena deposit and were present in a very small amount. The thermal stability ranges of the crystalline phases identified are summarized in Figure 4B.

Galena was stable up to 315°C and then began to slowly decrease until it disappears completely at 795°C. A melt coexisting with other crystalline compounds appeared at about 775°C (a melt is expected at 717°C in the system 70 wt% PbO-30 wt% SiO₂).¹⁰ With regard to the galena

weathering compounds, cerussite was stable up to 275°C decreasing from 275°C upwards and disappearing at 315°C. Massicot (PbO) appeared at 315°C increasing up to 475°C and completely disappearing at 595°C. Anglesite was stable up to 575°C, increasing between 575 and 775°C and afterward decreasing when it completely disappeared at 860°C. The reversible transformation between α-PbSO₄ and β-PbSO₄ at 883°C did not occur because the anglesite had already fully decomposed at a lower temperature (≈860°C) in our system. The appearance of lead oxysulfate, PbO·PbSO₄ (lanarkite),¹⁷ followed the decrease in galena (above 315°C) increasing progressively, but more quickly between 595 and 775°C. Lanarkite suddenly disappeared at 795°C, and a lead dioxy-sulfate, 2PbO·PbSO₄, formed. The lead dioxy-sulfate, 2PbO·PbSO₄, began to decrease at 900°C completely disappearing at 950°C. Minium (Pb₃O₄) formed between 810 and 860°C and was not found at 900°C. Meanwhile, a second melt developed; in fact, according to the PbO-PbSO₄ phase diagram, a sulfate melt should appear at this temperature.¹³ At 900°C, forsterite (Mg₂SiO₄) was also formed due to the reaction of the silica melt with the magnesia crucible. After cooling, the crystalline phases found were 2PbO·PbSO₄ and 4PbO·PbSO₄ crystallizing from the sulfate melt, quartz, and forsterite (Mg₂SiO₄).

In summary, the oxidation of galena (Figures 4 and 5) gave rise mainly to the formation of lanarkite, anglesite, and $2\text{PbO}\cdot\text{PbSO}_4$. In theory, anglesite is the first phase formed during the oxidation of galena.¹¹ However, this is only true at very low temperatures. According to other studies,¹⁴ lanarkite is actually the phase predominantly formed during the roasting of galena at 600°C .⁶ In our case, the anglesite determined was, in fact, already present in the original galena ore although some was also formed during the decomposition of galena between 600 and 800°C . The $\text{PbO}\text{--}\text{PbSO}_4$ phase diagram¹¹ indicates that both PbSO_4 and $\text{PbO}\cdot\text{PbSO}_4$ are stable at temperatures below 928°C when a sulfate liquid is formed. In contrast, in our case, a $\text{PbO}\text{--}\text{SiO}_2$ melt already developed at a lower temperature $\sim 775^\circ\text{C}$ and anglesite disappeared completely at $\sim 860^\circ\text{C}$. In addition, the $\text{PbO}\text{--}\text{PbSO}_4$ phase diagram also indicates that, on further oxidation, lanarkite and $2\text{PbO}\cdot\text{PbSO}_4$ should coexist. However, in our case, lanarkite decomposed completely at 795°C , while the lead dioxysulfate, $2\text{PbO}\cdot\text{PbSO}_4$, was formed which in turn decomposed at 950°C when a melt was formed. During the cooling, two lead oxysulfates, $2\text{PbO}\cdot\text{PbSO}_4$ and $4\text{PbO}\cdot\text{PbSO}_4$,

recrystallized from the melt; this is consistent with the $\text{PbO}\text{--}\text{PbSO}_4$ phase diagram where both compounds are stable below 863°C .¹¹ In fact, the presence of these lead oxysulfates indicates that a complete oxidation of galena into PbO was not obtained during the heating.

3.3 | Analysis of a misfired lead glaze

The misfired lead glaze exhibits three distinctive areas of different colors: opaque green, opalescent yellowish, and transparent honey, Figure 1. Figure 1A-C shows SEM BSE images corresponding to the green, yellow, and honey-colored areas, respectively. Three types of crystallites are observed in the three areas, and all of them contain mainly Pb and S (Figure 1D). Type I crystals appearing light gray are found only in the green glaze, Figure 1A. Type II crystals, which appear slightly darker in the SEM BSE images, show tabular or elongated sections of euhedral crystals. They also have a similar composition to Type I crystals, Figure 1D, and are found in both the green and the yellow glazes, Figure 1A,B. Type III crystals show a similar light gray color and share the tabular or elongated sections of

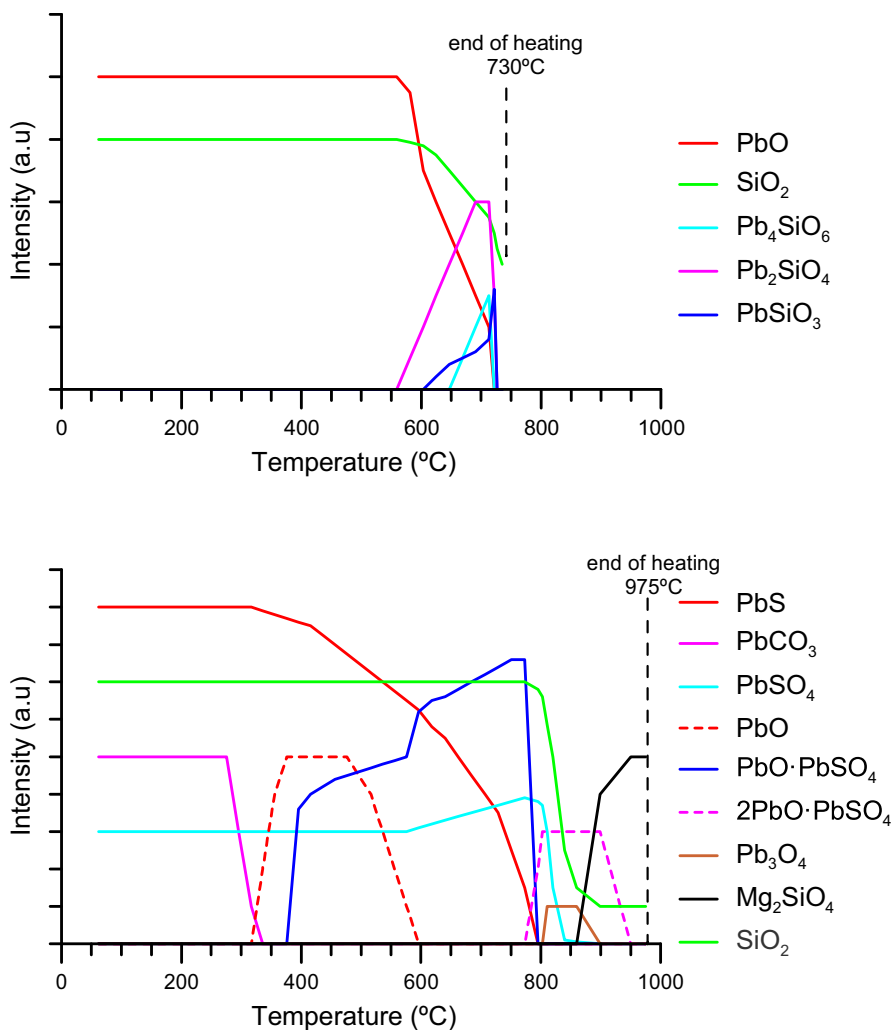


FIGURE 4 Thermal stability ranges of the crystalline phases identified for (A) $\text{PbO}\text{--}\text{SiO}_2$ and (B) $\text{PbS}\text{--}\text{SiO}_2$. The ordinate axis is obtained from the intensity of the principal peak of each crystalline phase relative to the intensity of the MgO crucible and gives a qualitative temperature evolution of each compound

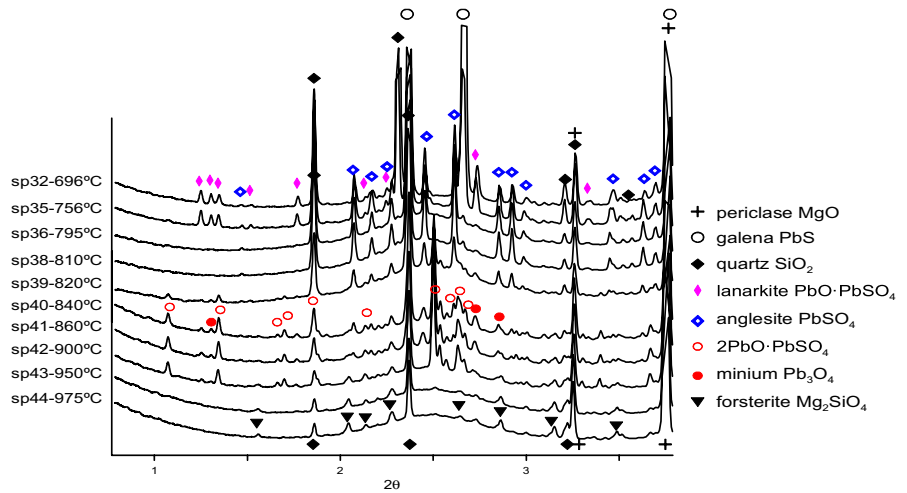


FIGURE 5 Selection of HT-SR-XRD patterns of the final firing stage for the mixture PbS-SiO₂

ehedral crystals as found in Type II. They are present in the three colored areas of the glaze, Figure 1. However, the chemical composition of Type III crystals is slightly different to those of Type II; they contain mainly Pb and S, but also some Cl, and minor amounts of Si and Ca, Figure 1D. Crystallites, Type II and Type III, show a similar atomic contrast in the BSE images. Quantitative chemical analysis of the crystallites is not possible with the EDS detector because of the large overlapping of S-K α , Pb-M α , and Cl-K α X-ray fluorescent peaks. Consequently, the chemical composition of the crystallites and the glaze is obtained by EPM, using a wavelength dispersive X-ray spectroscopy detector system (WDS) with a superior X-ray peak resolution and greater peak to background ratio. The chemical composition of the glaze in wt% is 73.5% PbO, 19.6% SiO₂, 1.5% Al₂O₃, 1.5% SO₃, 1.2% ZnO, 1.1% FeO, 0.5% Na₂O + K₂O, 0.2% CaO, and 0.05% Cl. The average and standard deviation of the various analyses made on the crystallites are shown in Table 1. Type I crystals contain 86.1 wt% Pb and 13.6 wt% S and no O, corresponding to galena. Type II and Type III crystallites are identified by SR- μ XRD as lanarkite, PbO·PbSO₄, and mattheddleite, a lead silicate sulfate chloride¹⁸⁻²⁰ of composition Pb₁₀(SiO₄)_{3.5}(SO₄)₂Cl₂, respectively, as shown in Figure 6. The chemical composition obtained for the Type II crystals is also in good agreement with those of lanarkite, PbO·PbSO₄. Conversely, the chemical composition determined for the Type III crystallites (Ca_{0.04}Pb_{0.96})₁₀(SiO₄)₄(SO₄)₂Cl_{0.8} differs from the theoretical composition;

contains less Cl, some unexpected Ca, and unbalanced Si and S. In fact, mattheddleite is a rare mineral of the apatite supergroup (ellestadite) of theoretical composition Pb₅(SiO₄)_{1.5}(SO₄)_{1.5}(Cl,OH)²¹; the other endmembers of this group are hydroxyllelestadite and fluorellestadite of theoretical composition Ca₅(SiO₄)_{1.5}(SO₄)_{1.5}(OH) and Ca₅(SiO₄)_{1.5}(SO₄)_{1.5}F, respectively.²⁰ Consequently, calcium may also be incorporated in the structure. The unbalanced Si and S measured by EPM were already noticed and associated to large and inaccurate absorption corrections occurring when celestite is used as S standard.²¹ In fact, our data are in good agreement with other mattheddleite EPM analysis. In our case, the neoformed inclusions of mattheddleite integrated available elements from the surrounding environment (glaze) during crystallization and, particularly, incorporated some calcium. The gangue also included some sphalerite grains that explain the presence ZnO in the glaze.

Under the optical microscope (Figure 7), galena is easily recognizable in reflected light, Figure 7C, by its high reflectance and because of the fractures along the cubic planes of exfoliation of some grains. Lanarkite and mattheddleite can be distinguished with crossed polarized light (XPL); lanarkite displays 2nd/3rd-order interference colors and inclined extinction (birefringence = 0.108), while mattheddleite has straight extinction and 1st and low 2nd-order interference colors (birefringence = 0.018), Figure 7B. In addition, some tabular sections of lanarkite show polysynthetic twins. In reflected light, lanarkite

TABLE 1 Average and standard deviation (in parenthesis) of the chemical composition of the crystallites measured by electron microprobe

wt%	N	Pb	S	Si	Cl	Ca	O	Sum
Type I	6	86.1 (0.3)	13.6 (0.1)	—	—	—	—	99.7 (0.3)
Type II	8	78.1 (0.8)	5.5 (0.1)	0.2 (0.2)	—	0.1 (0.1)	14.6 (0.2)	98.5 (1.1)
Type III	9	75.1 (0.5)	2.5 (0.1)	4.5 (0.3)	1.2 (0.2)	0.7 (0.1)	14.9 (0.2)	98.8 (0.3)

The oxygen is calculated by stoichiometry.

N, number of crystallites measured.

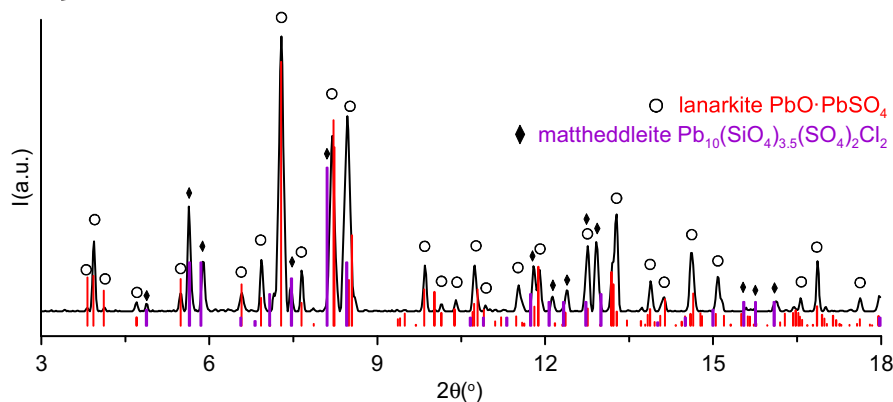


FIGURE 6 Synchrotron radiation micro-X-ray diffraction pattern of the crystallites in the misfired glazes. The reference patterns marked correspond to the JPDF database patterns 01-071-2069 for lanarkite and 00-041-0610 for mattheddleite

shows relief and a darker contrast than mattheddleite, Figure 7C.

The presence of different crystallites in the glaze is responsible for the various appearances and colors of the three areas: opaque green, translucent yellow, and transparent honey. The occurrence of galena grains accounts for the opacity, and the presence of Fe^{2+} ions dissolved in the glaze is most probably responsible for the green color. The concurrence of galena and Fe^{2+} is explained by the glaze exposure to a reducing atmosphere during the firing. The shortage of oxygen is responsible for both the delayed decomposition of galena and the reduction in the iron ions. A possible cause for this reducing atmosphere might be the exposure of the glazed surface to the flame. The opalescent yellow and the transparent honey areas would not have been exposed and, consequently, show the yellow tinge characteristic of Fe^{3+} and of lead glazes. Although both lanarkite and mattheddleite crystallites are present in the opalescent yellow area, lanarkite crystallites are responsible for the opalescence, as they have a pearly luster appearing

macroscopically translucent. The transparent honey area, however, contains only mattheddleite crystallites, which are transparent and show an adamantine luster.

4 | DISCUSSION

Although the first experimental studies of the PbO-SiO_2 system⁹ indicated that a series of compounds with $\text{PbO}:\text{SiO}_2$ mole ratios of 4:1, 3:1, 2:1, 1:1, and 5:8 were formed; only PbSiO_3 , Pb_2SiO_4 , and Pb_4SiO_6 were confirmed by other research.^{8,22} Moreover, Jak et al.²³ found that PbSiO_3 and Pb_2SiO_4 melt congruently, while Pb_4SiO_6 decomposes incongruently. Our high-temperature experiment is in perfect agreement with this. Moreover, the temperatures at which the different compounds form and decompose match our data, supporting the validity of our kinetic data.

On the other hand, based on the PbO-PbSO_4 phase diagram¹³ for temperatures lower than 860°C , anglesite (PbSO_4) and lanarkite (PbO-PbSO_4) are the two stable

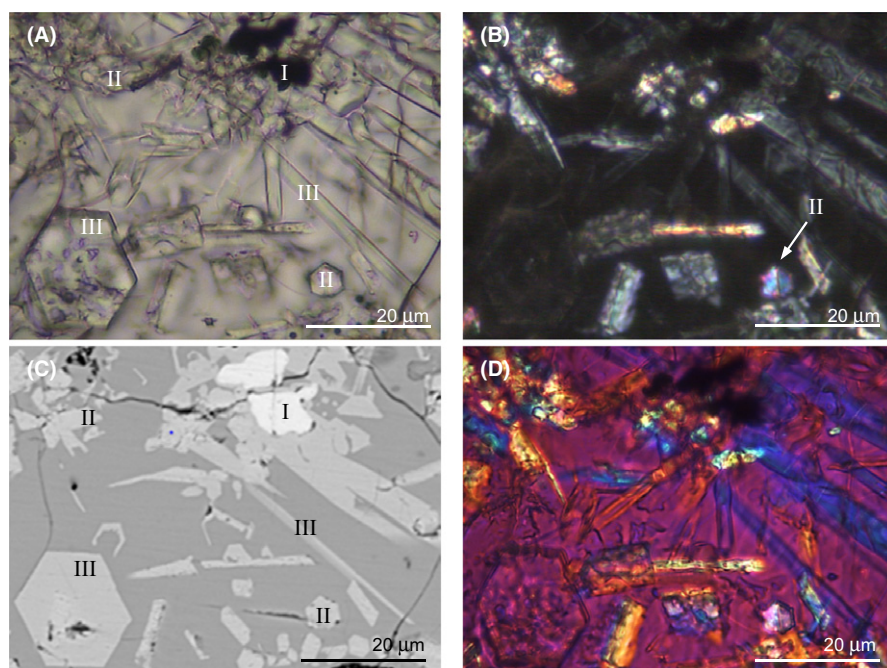


FIGURE 7 Optical microscopy images of the green area glaze. (A) PPL transmitted light showing opaque grains of galena (I), transparent crystals of lanarkite (II), and mattheddleite (III); (B) XPL transmitted light where the elongated section of the mattheddleite crystals shows a 1st-order gray color, and the hexagonal basal sections are extinguished: the elongated and prismatic sections of lanarkite exhibit 2nd/3rd-order interference colors; marked with an arrow, a twin; (C) reflected light, galena (I) appears very reflectant, mattheddleite (III) exhibits lower relief than lanarkite (II); (D) XPL transmitted light with $\frac{1}{4}$ lambda compensator

phases. Further oxidation tends to form lanarkite which leads to the subsequent development of first $2\text{PbO}\cdot\text{PbSO}_4$ and then $3\text{PbO}\cdot\text{PbSO}_4$.²⁴

In the $\text{PbS}\text{--}\text{SiO}_2$ system studied, lead silicates are not formed. The lack of lead silicates is probably due to remaining sulfates in the glaze mixture that handicapped the crystallization of the PbO/SiO_2 compounds. The oxidation of galena gives rise mainly to the formation of lanarkite ($\text{PbO}\cdot\text{PbSO}_4$) at a temperature as low as $\sim 315^\circ\text{C}$ disappearing suddenly at 795°C . The sudden disappearance of lanarkite in the $\text{PbS}\text{--}\text{SiO}_2$ system happens at lower temperatures than in the $\text{PbO}\text{--}\text{PbSO}_4$ system. This can be related to the presence of SiO_2 , which certainly plays a role, giving rise to a $\text{PbO}\text{--}\text{SiO}_2$ melt at $\sim 775^\circ\text{C}$. The green and yellow areas of the misfired glaze also show the presence of a silica melt and lanarkite, but not the compounds formed at higher temperatures. Anglesite is often present in the original galena ore as a weathering product and, considering that it is stable up to $\sim 860^\circ\text{C}$, it should be found in the misfired glaze. Therefore, the absence of anglesite could be an indicative that it was not present in the galena used by ancient potters.

The two basic lead sulfates, $2\text{PbO}\cdot\text{PbSO}_4$ and $4\text{PbO}\cdot\text{PbSO}_4$ which are formed after the lanarkite decomposition in the high-temperature experiment, are not found in the honey area of the historical lead glaze. In fact, the presence of both galena and lanarkite in the misfired glaze indicates not only a low firing temperature (below 795°C) but also a short firing. Moreover, the flame also produces a reducing atmosphere, which delays sulfur oxidation and sulfate decomposition. The green and yellow colors of the misfired areas also indicate the presence of reduced and oxidized iron, respectively. Therefore, we can also suppose that the lack of oxygen due to the direct hit of the flame in the area affected the oxidation of galena and lanarkite and the formation of the glaze. Conversely, the transparent honey glaze shows neither galena nor lanarkite. However, mattheddleite $\text{Pb}_5(\text{SiO}_4)_{1.5}(\text{SO}_4)_{1.5}(\text{Cl},\text{OH})$, with some calcium substituting the lead atoms, is identified. Mattheddleite occurs in oxidized zones of lead deposits, associated with lanarkite and anglesite, and its formation is driven by the presence of chlorine. The thin cross section shows the sequence of formation of the sulfate compounds in the glaze. Galena is found surrounded by lanarkite crystals, Figure 7A, while lanarkite is found inside mattheddleite crystals in the green area of the glaze, Figure 8. Therefore, the sequence of compounds formed during the oxidation of galena is, first lanarkite and then mattheddleite, provided chlorine is available in the surrounding glaze.

There are two possible sources for the chlorine found in the glazes; it formed part of the galena mineral or there was contamination during the firing. A very popular lead mineral extraction site in Catalonia is the Begur Coast, also known as the coast of the six lead mines.²⁵ The mines are often

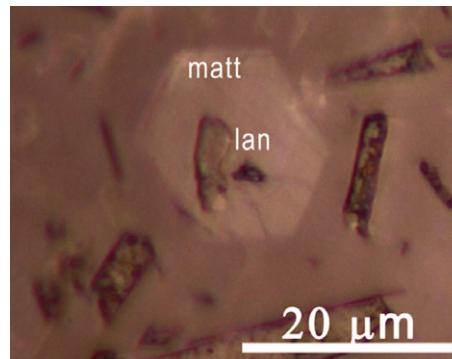


FIGURE 8 Optical microscopy image in reflected light of a lanarkite crystallite inside a crystal of mattheddleite

flooded by seawater, which could explain the presence of chlorine in the galena gangue. On the other hand, the ashes generated burning halophyte type plants^{26,27} during the firing could also provide chlorine to the surface of the glazes. In fact, the presence of ashes on the glaze surface during the firing could also explain the preferential direction of growth shown by the mattheddleite crystals—from the glaze surface toward the ceramic body—observed in the yellowish and honey areas of the glaze, Figure 1B,C.

The supposed disadvantage initially considered based on the $\text{PbO}\text{--}\text{PbSO}_4$ phase diagram, of the high temperatures at which the decomposition of the lead sulfates and formation of a melt ($\sim 928^\circ\text{C}$) happen is not correct for the system $\text{PbS}\text{--}\text{SiO}_2$. Our data show that, in the system $\text{PbS}\text{--}\text{SiO}_2$ at a temperature as low as 775°C , a melt is formed and that, at 795°C , the lanarkite is already fully decomposed. Nevertheless, adequate oxidation conditions are necessary to help the oxidative process take place. Consequently, optimal firing conditions for the $\text{PbS}\text{--}\text{SiO}_2$ system are a temperature only slightly higher than those of the $\text{PbO}\text{--}\text{SiO}_2$ system provided adequate oxidative conditions are guaranteed.

5 | CONCLUSIONS

The transformations during the production of a lead glaze with galena $\text{PbS}\text{--}\text{SiO}_2$ were studied by means of a HT-SR-XRD. The phase transformations and thermal stability of the compounds formed were determined, and the results obtained were compared to the available data for the $\text{PbO}\text{--}\text{SiO}_2$ and $\text{PbO}\text{--}\text{PbSO}_4$ systems. The oxidation of galena gives rise to the formation of lanarkite, $\text{PbO}\cdot\text{PbSO}_4$, at 315°C and its decomposition at 795°C , a temperature lower than those found in the $\text{PbO}\text{--}\text{PbSO}_4$ system (916°C). Moreover, in agreement with the $\text{PbO}\text{--}\text{PbSO}_4$ system, once lanarkite decomposes, two basic lead sulfates, $2\text{PbO}\cdot\text{PbSO}_4$ and $4\text{PbO}\cdot\text{PbSO}_4$, form. Lead silicates do not form in the $\text{PbS}\text{--}\text{SiO}_2$ system contrary to what is observed in the $\text{PbO}\text{--}\text{SiO}_2$

system where they form at temperatures above 750°C. The presence of lead sulfates in the silicate melt prevents the formation of the lead silicates. The results obtained show that the optimal firing conditions for the PbS–SiO₂ system are a temperature rather similar to the PbO–SiO₂ system, but when galena is used, highly oxidative conditions need to be guaranteed in order to eliminate sulfur from the glaze.

A historical misfired lead glaze still retaining relics of galena was also studied, and the crystalline phases developed were identified. Different color areas—green, yellow, and honey—showing different crystalline compounds of the glaze were discussed. Galena, lanarkite, PbO–PbSO₄, and mattheddleite, (Ca,Pb)₁₀(SiO₄)_{3.5}(SO₄)₂Cl₂, were identified. The crystallites are responsible for the opaque green (galena, lanarkite, and mattheddleite), opalescent yellow (lanarkite and mattheddleite), and transparent honey (mattheddleite) colors observed on the surface of the sample. The presence of galena and lanarkite indicates a maximum temperature of 795°C, although the reducing action of the flame could have delayed sulfur and sulfate oxidation even at higher temperatures. The crystallization of mattheddleite and its directional growth from the surface toward the glaze could be explained by the deposition of plant ashes on the glaze surface during the firing.

ACKNOWLEDGMENTS

Roberta Di Febo is grateful to the UVIC-UCC Scholarship Program, awarded by University of Vic, Central University of Catalonia. The authors are grateful to the project MAT2016-77753-R, 2017-2019 funded by the Ministerio de Ciencia e Innovación (Spain) and the ALBA Synchrotron Light Facility 2014060905 (BL04). Thanks are due to the project 2014SGR00581 (T.P.), 2014SGR1585 (J.M. and R.D.F.), and 2014SGR1661 (J.C.M.).

ORCID

Roberta Di Febo  <http://orcid.org/0000-0002-1102-8231>

Judit Molera  <http://orcid.org/0000-0003-3116-0456>

Trinitat Pradell  <http://orcid.org/0000-0002-8720-5492>

Joan C. Melgarejo  <http://orcid.org/0000-0001-7544-1191>

Oriol Vallcorba  <http://orcid.org/0000-0001-6499-7688>

REFERENCES

- Tite MS, Freestone I, Mason R, et al. Lead glazes in antiquity—methods of production and reasons for use. *Archaeometry*. 1998;40:241-260.
- Wood N, Freestone I. A Preliminary Examination of a Warring States Pottery Jar with So-Called “Glass Paste” Decoration. In Guo J, ed. *Science and Technology of Ancient Ceramics*: 3. *Proceedings of the International Symposium on Ancient Ceramics*. Shanghai, China: Shanghai Res. Soc. Sci. Technol. Ancient Ceram.; 1995:12-17.
- Wood N. *Chinese Glazes, the Origins, Chemistry and Re-Creation*. Philadelphia, PA: A&C Black London and University of Pennsylvania Press; 1999.
- Walton M, Tite MS. Production technology of Roman lead glazed pottery and its continuance into late antiquity. *Archaeometry*. 2010;52:733-759.
- Molera J, Pradell T, Salvadó N, et al. Lead Frits in Islamic and Hispano-Moresque Glazed Productions. In: Shortland AJ, Freestone IC, Rehren T, eds. *From Mine to Microscope: Advances in the Study of Ancient Technology*. Oxford: Oxbow Books; 2007:11-22.
- Gómez A, Gil C, Di Febo R, et al. Casa Convalescència (Vic, Osona): Aproximació arqueològica i arqueomètrica a un conjunt de vasos ceràmics del segle XVIII. In: *Actes III Jornades d'Arqueologia de la Catalunya Central*. Publicacions d'Arqueologia i Paleontologia 9; 2015:70-81.
- Lessler MA. Lead and lead poisoning from antiquity to modern times. *Ohio J Sci*. 1988;88:78-84.
- Geller RF, Creamer AS, Bunting EN. The system PbO–SiO₂. *J Res Nat Bur Stand*. 1934;13:237-244.
- Smart RM, Glasser FP. Compound formation and phase equilibria in the system PbO–SiO₂. *J Am Ceram Soc*. 1974;57:378-382.
- Factsage. Phase diagram PbO–SiO₂. http://www.crct.polymtl.ca/fact/phase_diagram.php?file=Pb-Si-O_PbO-SiO2.jpg&dir=FToxid. Accessed June 8, 2017.
- Eric RH, Timucin M. Phase equilibria and thermodynamics in the lead-lead sulphide system. *J S Afr Inst Min Metall*. 1969;88:353-361.
- Kullerud G. The lead-sulfur system. *Am J Sci*. 1969;267:233-256.
- Billhardt HW. New data on basic lead sulfates. *J Electrochem Soc*. 1970;117:690-692.
- Abdel-Rehim AM. Thermal and XRD analysis of Egyptian Galena. *J Therm Anal Calorim*. 2006;86:393-401.
- Hammersley P, Svensson SO, Hanfland M, et al. Two-dimensional detector software: from real detector to idealised image or two-theta scan. *High Press Res*. 1996;14:235-248.
- Fauth F, Peral I, Popescu C, et al. The new material science powder diffraction beamline at ALBA synchrotron. *Powder Diffr*. 2013;28:360-370.
- Richemond WE, Wolfe C. Crystallography of lanarkite. *Am Min*. 1938;23:799-804.
- Livingstone A, Ryback G, Fejer EE, et al. Mattheddleite, a new mineral of the apatite group from Leadhills, Strathclyde Region. *Scott J Geol*. 1987;23:1-8.
- Steele IM, Pluth JJ, Livingstone A. Crystal structure of mattheddleite: a Pb, S, Si phase with the apatite structure. *Min Mag*. 2000;64:915-921.
- Pasero M, Kampf AR, Ferraris C, et al. Nomenclature of the apatite supergroup minerals. *Eur J Mineral*. 2010;22:163-179.
- Essene EJ, Henderson CE, Livingstone A. The missing sulphur in mattheddleite, sulphur analysis of sulphates and paragenetic relations at Leadhills, Scotland. *Min Mag*. 2016;70:265-280.
- Calvert PD, Shaw RR. Liquidus behavior in the silica-rich region of the system PbO–SiO₂. *J Am Ceram Soc*. 1970;53:350-352.
- Jak E, Degterov S, Wu P, et al. Thermodynamic Optimization of the Systems PbO–SiO₂, PbO–ZnO, ZnO–SiO₂ and PbO–ZnO–SiO₂. *Metall Mater Trans B*. 1977;28:1011-1018.

24. Ponsot B, Salomon J, Walter P. RBS study of galena thermal oxidation in air with MeV O^{3+} ion beam. *Nucl Instr Meth Phys Res B*. 1998;136–138:1074-1079.
25. Perelló JMM. *Els minerals de Catalunya*. Barcelona: Institut d'Estudis Catalans; 1990.
26. Lynggaard F. *Tratado de cerámica*. Barcelona: Ediciones Omega; 1976.
27. Misra M, Raglund K, Baker A. Wood ash composition as a function of furnace temperature. *Biomass Bioenergy*. 1993;4:103-116.

How to cite this article: Di Febo R, Molera J, Pradell T, Melgarejo JC, Madrenas J, Vallcorba O. The production of a lead glaze with galena: Thermal transformations in the PbS–SiO₂ system. *J Am Ceram Soc*. 2017;00:1–11.
<https://doi.org/10.1111/jace.15346>